# Electron-phonon coupling in bcc and 9R lithium

Amy Y. Liu* and Marvin L. Cohen

*Department of Physics, University of California at Berkeley and Materials Sciences Division,
Lawrence Berkeley Laboratory, Berkeley, California 94720*

(Received 22 April 1991)

We test the hypothesis that the observed absence of superconductivity in Li results from weak electron-phonon coupling in the low-temperature 9R phase. A first-principles study of the phonon spectrum and electron-phonon coupling constant in bcc and 9R Li is presented. The electron-phonon coupling constant is found to be similar in bcc and 9R Li, and in both phases it is too strong to be consistent with the experimental upper bound on the superconducting transition temperature within the standard theory of phonon-mediated superconductivity.

## I. INTRODUCTION

Although Li is one of the simplest metals, some aspects of its electronic, structural, and superconducting properties remain as open problems. The simple electronic structure of atomic Li suggests that the metallic state should be describable by the nearly-free-electron picture. This, however, is not strictly the case. Band structure effects are more important in Li than in other alkali metals because of the strong Li pseudopotential. In addition, calculations[1,2] indicate that electron-phonon and electron-electron interactions are also significant in Li. All of these effects renormalize Fermi surface properties and cause deviations from the free electron model. Currently there is no formalism that allows all these effects to be treated on an equal footing.

A similar situation exists for studies of the crystal structure of Li. The low-temperature phase is complex and has been a subject of debate for many years. While Li crystallizes in the bcc structure at room temperature, it undergoes a martensitic phase transformation near 70 K. When this transformation was discovered over 30 years ago, the low-temperature phase was assigned to a faulted hcp structure.[3] In 1984, however, it was suggested[4] that the neutron scattering data[5] could be interpreted in terms of the rhombohedral 9R structure. This structure, shown in Fig. 1, consists of a close-packed lattice with a nine layer stacking sequence of ABABCBCAC. Recent neutron scattering data[6,7] indeed show that the low-temperature phase is predominantly 9R, but there is also evidence for the coexistence of some amount of bcc and other close-packed phases as well.

The uncertainty regarding the crystal structure of the low-temperature phase of Li may help explain another property of Li that is not well understood: the absence of a superconducting phase in the 1 K range. Since it is a simple metal, Li is expected to be well described by the conventional BCS theory of superconductivity, in which the electron pairing is phonon mediated. Calculations[1,8,9] of the electron-phonon coupling constant, $\lambda$, in bcc Li give a wide range of results, but the more reliable of these calculations generally yield a moderately large

value for $\lambda$ of about 0.4.[10] When this value of $\lambda$ is used in the McMillan equation[11] together with the conventional value for the Coulomb repulsion parameter $\mu^* = 0.1$ for simple metals, a superconducting transition temperature in the range of 1 K is obtained. This is in contradiction to experiment,[12] which shows Li to be a normal metal down to at least $T = 6$ mK.
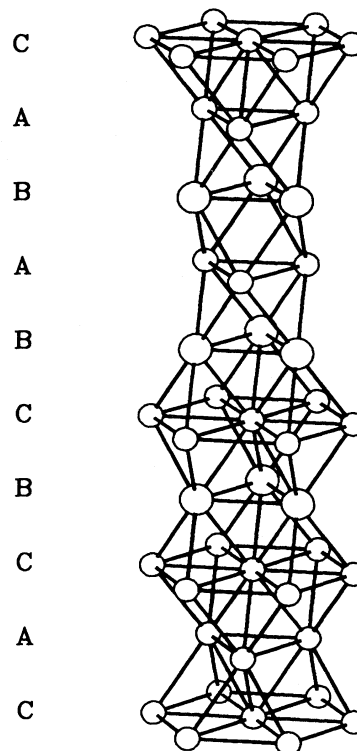


FIG. 1. The 9R crystal structure. The structure can be viewed as close-packed hexagonal layers with the stacking sequence ABABCBCAC. The primitive cell is rhombohedral with a basis of three atoms.

In this work we test the hypothesis that the absence of superconductivity in Li is due to a weak electron-phonon interaction in the low-temperature phase, which is predominantly 9R. Thus far, calculations of $\lambda$ in Li have focused on the room temperature bcc structure. These calculations have employed either empirical pseudopotential methods using the rigid ion approximation,[1] or all electron methods within the rigid muffin-tin approximation,[8,9] where the crystal potential is assumed to shift rigidly with phonon-induced atomic displacements. The phonon spectrum used in these calculations is either obtained from experiment or calculated using simplified models. Here we calculate the phonon spectrum and electron-phonon coupling parameter for both bcc and 9R Li, using an approach that goes beyond the rigid ion approximation. The change in the crystal potential induced by atomic displacements is self-consistently determined, and the electronic structure and phonon spectrum are both computed from first principles. The calculational method is discussed in Sec. II. Our results, presented in Sec. III, indicate that while $\lambda$ is smaller in 9R than in bcc Li, it is not small enough to be consistent with a superconducting transition temperature of less than 6 mK. The effects of electron-electron many-body interactions that are not included in our calculations but that are believed to be of some importance in Li are explored.

## II. METHOD

Electronic and vibrational properties are calculated using the first-principles pseudopotential total energy approach.[13,14] For a given phonon with wave vector $\mathbf{q}$ and mode $v$, the total energy, electronic wave functions, eigenvalues, and crystal potential are calculated for two different structures: the perfect crystal and a distorted lattice with phonon-induced atomic displacements frozen in. Within the harmonic approximation, the phonon frequency, $\omega_{\mathbf{q}v}$, is proportional to the square root of the energy difference between the two structures. The wave functions and crystal potentials obtained from the frozen phonon calculation allow the evaluation of the electron-phonon matrix element.

The standard definition[10] for the electron-phonon matrix element for scattering of an electron from state $n\mathbf{k}$ to state $n'\mathbf{k}'$ by a phonon $\mathbf{q}v$ is

$$g(n\mathbf{k},n'\mathbf{k}',\mathbf{q}v)= \left[\frac{\hbar\Omega_{\mathrm{BZ}}}{2M\omega_{\mathbf{q}v}}\right]^{1/2} \left\langle \psi^0_{n\mathbf{k}} \left| \hat{\epsilon}_{\mathbf{q}v}\cdot\frac{\delta V}{\delta\mathbf{R}} \right| \psi^0_{n'\mathbf{k}'} \right\rangle$$
$$\times\delta(\mathbf{k}-\mathbf{k}'-\mathbf{q}),\qquad(1)$$

where $\Omega_{\mathrm{BZ}}$ is the volume of the Brillouin zone, $M$ is the atomic mass, $\hat{\epsilon}_{\mathbf{q}v}$ is the phonon polarization vector, and $\delta V/\delta\mathbf{R}$ is the self-consistent change of the crystal potential caused by the phonon distortion. Previous studies of the electron-phonon interaction in Li have all been based on the rigid ion or rigid muffin tin approximation, in which the quantity $\delta V/\delta\mathbf{R}$ is replaced by the gradient of a non-self-consistent rigid potential. In the present work, we go beyond this approximation by calculating the crystal potential caused by phonon distortions self-consistently. The change in the potential is given by

$$\hat{\epsilon}_{\mathbf{q}v}\cdot\frac{\delta V}{\delta\mathbf{R}} = \frac{V_{\mathbf{q}v}-V_0}{\bar{u}_{\mathbf{q}v}},\qquad(2)$$

where $V_{\mathbf{q}v}$ and $V_0$ are the self-consistent crystal potentials for the distorted and undistorted crystals, respectively, and $\bar{u}_{\mathbf{q}v}$ is the root-mean-square phonon amplitude.

To calculate the electron-phonon coupling constant, $\lambda$, we expressed it as a sum over contributions from different modes and an average over wave vectors of a wave-vector and mode-dependent $\lambda_{\mathbf{q}v}$:[14]

$$\lambda=\sum_v(\Omega_{\mathrm{BZ}})^{-1}\int d^3q\,\lambda_{\mathbf{q}v}.\qquad(3)$$

The wave-vector-dependent coupling constant is given by

$$\lambda_{\mathbf{q}v}=2N(E_F)\frac{\langle\!\langle|g(n\mathbf{k},n'\mathbf{k}',\mathbf{q}v)|^2\rangle\!\rangle}{\hbar\omega_{\mathbf{q}v}},\qquad(4)$$

where $N(E_F)$ is the electronic density of states at the Fermi level, and $\langle\!\langle|g|^2\rangle\!\rangle$ is a Fermi surface average of the square of the electron-phonon matrix element.

The use of supercells in the frozen phonon method imposes the limitation that the wave vector $\mathbf{q}$ must be commensurate with the reciprocal lattice of the undistorted crystal. The condition simplifies the evaluation of $\langle\!\langle|g^2|\rangle\!\rangle$ since the $\delta$ function in Eq. (1) is satisfied automatically.[14] However, because the computational expense of plane wave based pseudopotential approaches grows quickly with the number of atoms in the supercell, it is not feasible to calculate $\lambda_{\mathbf{q}v}$ for more than a few wave vectors in the Brillouin zone. Hence the accuracy of the present calculation of $\lambda$ is limited by the sparse sampling of wave vectors in the Brillouin zone.

## III. RESULTS AND DISCUSSION

The calculated zero temperature total energies of bcc and 9R Li are plotted as a function of volume in Fig. 2. The two phases lie extremely close to energy. While our calculation finds the 9R structure to be slightly favored, the energy difference of about 0.1 mRy/atom is within the uncertainty inherent in the calculation. We have also calculated the total energies of Li in the fcc and hcp structures and find that these phases also lie within a fraction of a mRy of bcc and 9R Li. The proximity of all these phases is consistent with the observation that at low temperatures Li consists of a mixture of several different structural phases.[7]

The minimum in the total energy curve of bcc Li lies at a volume of 131 a.u./atom. Although this is about 8% smaller than the experimental value for the equilibrium volume,[15] the inclusion of zero point motion corrections to the calculated zero temperature equation of state shifts the equilibrium volume up and results in reasonable agreement with experiment.[16] In the remainder of this work, calculations for both the bcc and 9R structures are carried out at a volume of 142.52 a.u./atom, which is the experimentally determined volume at 78 K.[6] Since the measured $c/a$ ratio in 9R Li corresponds to the ideal close packing value to within 0.1%,[6] the ideal value is assumed.

The calculated electronic band structures of bcc and
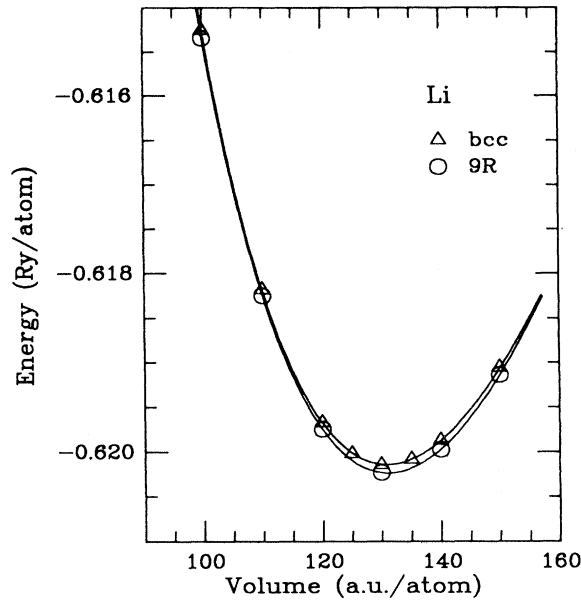
FIG. 2. Calculated total energy vs volume for bcc and 9R Li. The triangles and circles are the calculated points for the bcc and 9R structures, respectively, and the curves are fits to the Birch-Murnaghan equation of state.

FIG. 3. Calculated band structures for (a) bcc and (b) 9R Li. Energies are measured relative to the Fermi level. The 9R symmetry points are labeled as in Ref. 17.

9R Li are shown in Fig. 3. The symmetry points in the 9R Brillouin zone are labeled as in Ref. 17. It has been suggested[18] that Fermi surfaces of the bcc and 9R phases may be qualitatively different in that the bcc Fermi surface does not contact the Brillouin zone, while the 9R Fermi surface may. It was speculated[18] that this effect could lead to significant differences in the electronic density of states at the Fermi level, and hence differences in the electron-phonon coupling parameter $\lambda$. While the Fermi surface of 9R Li calculated within the local density approximation indeed shows contact with the Brillouin zone near the L point, the value of the density of states near the Fermi level does not differ much from that of bcc Li. The band masses we obtain from the densities of states at the Fermi level are $m_b = 1.63m$ and $1.75m$ for bcc and 9R Li, respectively, where $m$ is the electron mass.

For the phonon frequencies and electron-phonon cou-

pling constant in bcc Li, three $\mathbf{q}$ points in the Brillouin zone are considered: $P$, $H$, and $N$. The polarization vectors for phonons with these wave vectors are determined by symmetry and correspond to simple longitudinal and transverse modes. The results for $\omega_{\mathbf{q}\nu}$ and $\lambda_{\mathbf{q}\nu}$ are listed in Table I. The calculated phonon frequencies agree with the measured $T = 98$ K values to within a few percent.[19] While most of the phonon modes considered are found to be harmonic, the phonon force constant of the soft transverse mode at $N$ is found to depend on the amplitude of the phonon displacement used in the frozen phonon calculation. The results shown in Table I correspond to an

TABLE I. Calculated electron-phonon coupling parameters and calculated and experimental phonon frequencies for bcc Li. The experimental values are from Ref. 19. The phonon polarization is indicated by L for longitudinal and T for transverse. At both the $H$ and $P$ points, the longitudinal and two transverse modes are all degenerate.

| $\mathbf{q}\nu$ | $\lambda_{\mathbf{q}\nu}$ | $\omega_{\mathbf{q}\nu}$ ($10^{13}$ rad/s) | $\omega_{\mathbf{q}\nu}^{\text{expt}}$ ($10^{13}$ rad/s) |
|---|---|---|---|
| $N$ (L) | 0.10 | 5.51 | 5.68 |
| $N$ ($T_z$) | 0.21 | 3.52 | 3.63 |
| $N$ ($T_{xy}$) | 0.94 | 1.15 | 1.24 |
| $H$ (LT) | 0.00 | 5.86 | 5.57 |
| $P$ (LT) | 0.09 | 4.65 | 4.41 |

amplitude that yields a phonon frequency in agreement with experiment. Averaging the calculated $\lambda_{qv}$ leads to $\lambda = 0.51$. We have tested the effect of including more wave vectors in the Brillouin zone average of $\lambda_{qv}$ and find that it does not change the results significantly.[20] From these tests, we estimate an uncertainty of $\pm 0.08$ in the calculated $\lambda$. The present result for $\lambda$ in bcc Li is on the high end of the range spanned by earlier calculations,[1,8,9] but since there are large uncertainties in all these calculations, a difference of 20% is not unexpected. Furthermore, calculations based on the rigid ion approximation tend to underestimate $\lambda$ in other simple metals such as Al,[21] so it is not surprising that the earlier estimates of $\lambda$ based on this approximation are generally smaller than the present result.

For the 9R structure, which contains three atoms per unit cell, the $\Gamma$, T, and L points in the Brillouin zone are sampled. The phonon polarization vectors for some of the phonon modes at these wave vectors are not determined by symmetry. In these cases, the Hellmann-Feynman forces due to atomic displacements in the supercell are calculated. This allows computation of the dynamical matrix, which is then diagonalized to yield the phonon polarization vectors. The calculated frequencies and electron-phonon coupling parameters are listed in Table II. While there are no experimental data for the phonon spectrum of 9R Li, there is one model calculation[17] to which we can compare our results for $\omega_{qv}$. That calculation employed a pseudopotential model, with parameters fit to the phonon spectrum of bcc Li. The

present first-principles calculation yields phonon frequencies that are in good agreement with the model calculation. Averaging the contributions to $\lambda$ from the three q points yields $\lambda = 0.41$ for 9R Li.

It is interesting to compare the results for the two structures of Li. For the limited number of wave vectors considered in this work, the range of calculated phonon frequencies is similar in the two phases. In addition, the earlier model calculation,[17] which studied the 9R and bcc phonon spectra along several symmetry directions, found the overall frequency distributions of bcc and 9R phonons to be similar. One of the unusual features of the bcc spectrum is the soft transverse mode at $N$ polarized in the $[1\bar{1}0]$ direction. Because of the orientational relation maintained between the bcc and 9R structures, the bcc $\Gamma$ to $N$ and the 9R $\Gamma$ to $T$ lines point along the same direction in reciprocal space. An inspection of Table II reveals soft transverse phonon modes at $T$ in the 9R phase as well. Hence the phonon frequencies for corresponding branches do not seem to be strongly affected by the bcc-9R transition. Because of the similarities between the phonon spectrum of the 9R and bcc phases, and also between the electronic density of states as discussed earlier, it is not surprising that the electron-phonon interaction is comparable in the two phases.

To calculate the superconducting transition temperature, estimates for the average phonon frequency, $\langle \omega \rangle$, and the Coulomb repulsion parameter, $\mu^*$, are needed. The average phonon frequency, which is given by $(\sum_{q,v} \lambda_{qv} \omega_{qv})/(\sum_{q,v} \lambda_{qv})$, is found to be 200 K for 9R Li

TABLE II. Calculated electron-phonon coupling parameters and phonon frequencies for 9R Li. The model calculation results for the frequencies are from Ref. 17. The phonon modes are labeled by the irreducible representation to which they belong, and the degeneracies of the modes are listed in parentheses.

| $qv$ | $\lambda_{qv}$ | $\omega_{qv}$ ($10^{13}$ rad/s) | $\omega_{qv}^{\text{model}}$ ($10^{13}$ rad/s) |
|---|---|---|---|
| $\Gamma_{3u}$ (2) | 0.060 | 1.97 | 2.1 |
| $\Gamma_{3g}$ (2) | 0.026 | 1.84 | 2.1 |
| $\Gamma_{2u}$ (1) | 0.048 | 4.59 | 5.0 |
| $\Gamma_{1g}$ (1) | 0.047 | 4.53 | 5.0 |
| $T_{1g}$ (1) | 0.080 | 2.80 | 2.9 |
| $T_{3g}$ (2) | 0.092 | 1.16 | 1.3 |
| $T_{2u}$ (1) | 0.055 | 5.41 | 5.8 |
| $T_{2u}$ (1) | 0.090 | 2.89 | 2.9 |
| $T_{3u}$ (2) | 0.057 | 2.25 | 2.5 |
| $T_{3u}$ (2) | 0.092 | 1.17 | 1.3 |
| $L_{1g}$ (1) | 0.023 | 3.96 | 3.9 |
| $L_{1u}$ (1) | 0.026 | 2.39 | 2.4 |
| $L_{1u}$ (1) | 0.026 | 3.93 | 3.9 |
| $L_{2g}$ (1) | 0.020 | 4.63 | 4.3 |
| $L_{2g}$ (1) | 0.017 | 5.58 | 5.5 |
| $L_{2u}$ (1) | 0.045 | 2.95 | 2.8 |
| $L_{2u}$ (1) | 0.036 | 3.93 | 3.9 |
| $L_{2u}$ (1) | 0.032 | 5.37 | 5.5 |
| $L_{2u}$ (1) | 0.017 | 5.81 | 5.8 |

and 180 K for bcc Li. A realistic calculation of $\mu^*$ requires a knowledge of the wave-vector- and frequency-dependent dielectric function in the solid, and this parameter is usually approximated through scaling model calculations and experimental data. If the dielectric function in Li is approximated by the static Thomas-Fermi expression, then a value of $\mu^*=0.12$ is obtained. This is consistent with most estimates for $sp$ metals. Using the calculated values of $\langle \omega \rangle$, $\lambda$, and $\mu^*$ in the McMillan equation, we obtain superconducting transition temperatures in the range of 1 K for both $9R$ and bcc Li (Table III). Even if we allow for uncertainties of $\pm 0.08$ in $\lambda$ and $\pm 0.02$ in $\mu^*$, we still find $T_c$ to be higher than the experimental limit of 6 mK. This can be seen in Fig. 4, where isotherms of $T_c$ for $9R$ Li are plotted in the $(\lambda, \mu^*)$ plane. There is no overlap between the oval, which indicates the estimated range of parameters allowed for $9R$ Li, and the region of parameter space corresponding to $T_c < 6$ mK. Thus while the electron-phonon interaction is calculated to be slightly weaker in the low-temperature $9R$ phase, the difference is not sufficient to account for the observed absence of superconductivity in Li.

In addition to estimating $T_c$, we can use the calculated values of $\lambda$, along with the calculated electronic density of states, to estimate the thermal mass of Li. In the first column of Table IV, we list calculated thermal masses assuming that the mass enhancement comes only from band structure and electron-phonon effects $[m_{th}=m_b(1+\lambda)]$. For both the bcc and $9R$ phases, the thermal mass is calculated to be about 10% larger than the value of $m_{th}/m=2.23\pm0.05$ obtained from measurements of the low-temperature specific heat in Li.[22] Hence both the specific heat data and the experimental upper limit on $T_c$ suggest that the calculated values of $\lambda$ are too large.

Thus far we have considered only band structure
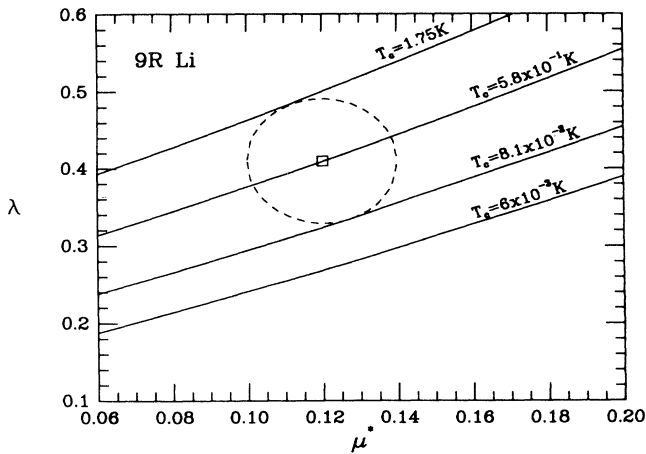


FIG. 4. $\lambda$ vs $\mu^*$ for $9R$ Li. The square represents the calculated values of $\lambda$ and $\mu^*$, and the dashed line indicates the estimated uncertainties in these parameters. The solid curves are $T_c$ isotherms calculated from the McMillan equation.

TABLE III. Calculated band mass, average phonon frequency, average electron-phonon coupling parameter, and superconducting transition temperatures for bcc and $9R$ Li. A value of $\mu^*=0.12$ is assumed, and $\lambda_{sp}$ is taken to be 0.1 in calculations of $T_c^{sp}$.

|     | $m_b/m$ | $\langle \omega \rangle$ (K) | $\lambda$ | $T_c$ (K) | $T_c^{sp}$ (K) |
| --- | --- | --- | --- | --- | --- |
| bcc | 1.63 | 180 | 0.51 | 1.73 | 0.18 |
| $9R$ | 1.75 | 200 | 0.41 | 0.58 | 0.0088 |

effects and the electron-phonon interaction in Li. As mentioned earlier, other many-body effects are believed to be important in Li as well. For example, electron gas calculations[2] at densities corresponding to Li indicate that while electron-electron self-energy corrections do not lead to a large mass enhancement factor $(1+\lambda_{ee} \approx 1.06)$, they do result in a renormalization factor that is significantly reduced from unity $[Z_{ee}(k_F) \approx 0.65]$. When both electron-electron and electron-phonon effects are included, the thermal mass is given by

$$m_{th}=m_b \left| \frac{1-\partial \Sigma_{ee}/\partial \omega - \partial \Sigma_{ep}/\partial \omega}{1+\partial \Sigma_{ee}/\partial \epsilon_p + \partial \Sigma_{ep}/\partial \epsilon_p} \right|_{\omega=0, p=p_f}, \quad (5)$$

where $\Sigma_{ee}(\omega,p)$ and $\Sigma_{ep}(\omega,p)$ are the electron-electron and electron-phonon self-energies.[10] With the usual assumption that $\Sigma_{ep}$ has only weak momentum dependence,[10] we can rewrite this as

$$m_{th}=m_b(1+\lambda_{ee})[1+Z_{ee}(k_F)\lambda] . \quad (6)$$

Since it is computationally expensive to calculate the renormalization factor and quasiparticle band mass for a real metal, we use instead the band masses calculated within the local density approximation, together with the electron-gas results[2] for the electron-electron effects. As shown in the second column of Table IV, this gives $m_{th}=2.30m$ and $2.35m$ for bcc and $9R$ Li, respectively. Hence because the renormalization factor in Li is expected to be significantly smaller than one, the inclusion of electron-electron effects brings the calculated mass enhancement factor into reasonable agreement with the specific heat measurements. Unfortunately, the question of how the reduced quasiparticle weight might affect superconductivity has not been examined.

TABLE IV. Calculated thermal masses, for bcc and $9R$ Li, including contributions from electron-phonon ($ep$), electron-electron ($ee$), and spin fluctuation ($sp$) effects. Electron-electron and spin fluctuation parameters are taken from Refs. 2 and 9, respectively. The masses are listed in units of the electron mass.

|     | $ep$ | $ep+ee$ | $ep+sp$ | $ep+ee+sp$ |
| --- | --- | --- | --- | --- |
| bcc | 2.46 | 2.30 | 2.62 | 2.41 |
| $9R$ | 2.47 | 2.35 | 2.64 | 2.47 |
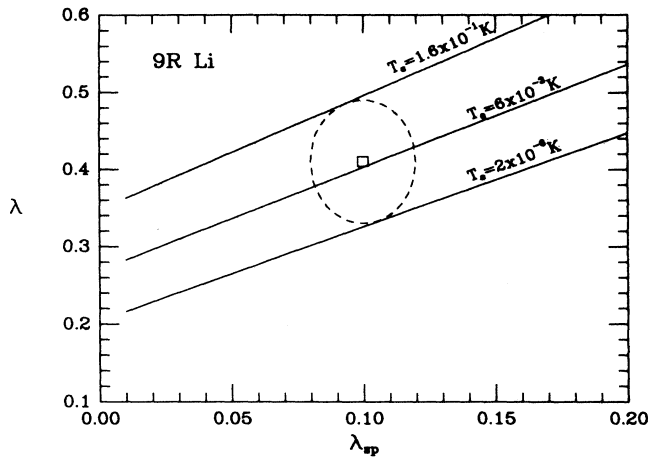
FIG. 5. $\lambda$ vs $\lambda_{sp}$ for 9R Li. The square represents our best estimates for $\lambda$ and $\lambda_{sp}$, based on this work and Ref. 9, and the dashed line indicates the uncertainties in these parameters. The solid curves are $T_c$ isotherms calculated from Eq. (7), assuming $\mu^* = 0.12$.

In addition to the spin-symmetric electron correlations considered above, spin fluctuations, or paramagnons, may also be important in Li. It has been suggested[9] that the calculated values of $\lambda$ for Li are reliable, but that spin fluctuations are responsible for suppressing electron pairing and superconductivity. If the characteristic energy scale of the paramagnons is small compared to $E_f$, the superconducting transition temperature can be estimated from

$$T_c = \frac{\langle \omega \rangle}{1.2} \exp \left[ \frac{-1.04(1+\lambda+\lambda_{sp})}{\lambda - \mu^*(1+0.62\lambda) - \lambda_{sp}} \right] , \qquad (7)$$

where $\lambda_{sp}$ is the mass enhancement parameter due to spin fluctuations.[23] In expressions for the thermal mass, $\lambda$ should be replaced by $\lambda + \lambda_{sp}$. Spin-polarized local density calculations[9] yield a mass enhancement factor due to paramagnons of about $1 + \lambda_{sp} = 1.1$ in bcc and hcp Li. Assuming $\lambda_{sp} = 0.1$ for 9R Li as well, we find that spin fluctuations reduce the predicted superconducting transition temperatures of 9R and bcc Li to 0.0088 and 0.19 K, respectively. In Fig. 5, we have plotted $T_c$ isotherms for

9R Li in the $(\lambda, \lambda_{sp})$ plane, assuming $\mu^* = 0.12$. Although our best estimate for $T_c$ in 9R Li is higher than the experimental limit, there is a large area of overlap between the oval indicating the uncertainty in the calculated parameters and the $T_c < 6$ mK region. The corresponding region of overlap for bcc Li (not shown) is much smaller, but with $\lambda_{sp} = 0.1 \pm 0.02$, it is possible to suppress the predicted $T_c$ for the bcc phase below the experimental limit as well. However, if spin fluctuations are indeed important, they should contribute to the enhancement of the electronic density of states at the Fermi level, and as already noted, the electron-phonon and electron-electron effects are sufficient to account for the enhancement determined from low-temperature specific heat measurements. As shown in Table IV, adding the contribution from spin fluctuations leads to somewhat worse agreement.

In summary, we have calculated the electron-phonon coupling parameter in both the room temperature and low-temperature phases of Li. Our results indicate that the electron-phonon interaction in Li is not strongly structure dependent, and in both phases, it is sufficiently strong to suggest a superconducting transition in the range of 1 K. The reason for the observed absence of superconductivity in Li down to 6 mK remains an open problem. While including the effects of spin fluctuations may suppress the calculated $T_c$ below the experimental limit, it also results in large discrepancies between the calculated and measured thermal masses. Electron-electron correlation effects reduce this discrepancy, but the difference is still significant. We believe that further calculations investigating the role of these many-body interactions in Li would be useful.

## ACKNOWLEDGMENTS

*Present address: Complex Systems Theory Branch, Naval Research Laboratory, Washington, D.C. 20375.

[1]P. B. Allen and M. L. Cohen, Phys. Rev. 187, 525 (1969).

[2]J. E. Northrup, M. S. Hybertsen, and S. G. Louie, Phys. Rev. B 39, 8198 (1989).

[3]G. S. Barrett, Acta Crystallogr. 9, 671 (1956).

[4]A. W. Overhauser, Phys. Rev. Lett. 53, 64 (1984).

[5]C. M. McCarthy, C. W. Tompson, and S. A. Werner, Phys. Rev. B 22, 574 (1980).

[6]H. G. Smith, Phys. Rev. Lett. 58, 1228 (1987).

[7]W. Schwarz and O. Blaschko, Phys. Rev. Lett. 65, 3144 (1990).

[8]D. A. Papaconstantopoulos, L. L. Boyer, B. M. Klein, A. R. Williams, V. L. Moruzzi, and J. F. Janak, Phys. Rev. B 15, 4221 (1977).

[9]T. Jarlborg, Phys. Scr. 37, 795 (1988).

[10]G. Grimvall, The Electron-Phonon Interaction in Metals (North-Holland, Amsterdam, 1981).

[11]W. L. McMillan, Phys. Rev. 167, 331 (1968).

[12]T. L. Thorp, B. B. Triplett, W. D. Brewer, M. L. Cohen, N. E. Phillips, D. A. Shirley, J. E. Templeton, R. W. Stark, and P. H. Schmidt, J. Low Temp. Phys. 3, 589 (1970).

[13]J. Ihm, A. Zunger, and M. L. Cohen, J. Phys. C 12, 4409

(1979); **13**, 3095 (E) (1980).

[14]P. K. Lam, M. M. Dacorogna, and M. L. Cohen, Phys. Rev. B **34**, 5065 (1986).

[15]C. Kittel, *Introduction to Solid State Physics,* 6th ed. (Wiley, New York, 1986).

[16]M. M. Dacorogna and M. L. Cohen, Phys. Rev. B **34**, 4996 (1986).

[17]Y. R. Wang and Q. W. Overhauser, Phys. Rev. B **34**, 8401 (1986).

[18]N. W. Ashcroft, Phys. Rev. B **39**, 10552 (1989).

[19]W. Kress, *Phonon Dispersion Curves, One-Phonon Densities of State, and Impurity Vibrations of Metallic Systems* (Fachinformations-Zentrum Karlsruhe, Eggenstein-Leopoldshafen, 1987).

[20]R. G. Dandrea (private communication).

[21]H. Rietschel, Z. Phys. B **30**, 271 (1978).

[22]N. E. Phillips, CRC Crit. Rev. Solid State Sci. **2**, 467 (1971).

[23]G. Gladstone, M. A. Jensen, and J. R. Schrieffer, in *Superconductivity,* edited by R. D. Parks (Dekker, New York, 1969), Vol. 2, p. 665.